3D anisotropic modelling of deep drifts at the Meuse/Haute-Marne URL

Mountaka Souley, Ngoc Minh Vu, Gilles Armand

3D anisotropic modelling of deep drifts at the Meuse/Haute-Marne URL

M. Souley[1], M.N. Vu[2] & G. Armand[3]
[1] *Ineris, Ecole des Mines, Campus ARTEM, 54042 Nancy, France*
[2] *Andra R&D, 92298 Chatenay-Malabry, France*
[3] *Andra, Meuse/Haute-Marne Underground Research Laboratory, 55290 Bure, France*

1 INTRODUCTION

The Callovo-Oxfordian (COx) claystone is considered as a potential geological host formation for high-level and intermediate-level long-lived radioactive wastes in France. In 2000, the French National Radioactive Waste Management Agency (Andra) began to build an Underground Research Laboratory (URL) at Meuse/Haute-Marne in order to demonstrate the feasibility of a geological repository in the COx formation. The excavation of galleries at the main level (490 m depth) of the URL, essentially following two directions of in-situ minor (σ_h) and major (σ_H) horizontal stresses, shows a significant anisotropy of the excavation induced fractured zones (Armand et al 2014). Different factors contribute probably to this anisotropic response of the COx to the excavation operation, such as inherent anisotropy of the stiffness and strength, anisotropic initial stresses, excavation induced anisotropic pore pressure repartition, excavation induced instability of quasi-brittle rock, etc.

The benchmark "Transverse action" consists in developing numerical models to characterize the COx behavior and using them for modeling the COx response due to the excavation. In the framework of this benchmark, different models, such as anisotropic elasto-visco-plastic models incorporating with non-local or second gradient modeling, anisotropic elastic-damage model, discrete modeling, have been proposed to successful reproduce the excavation induced fractured zones and the convergence measurement for both drifts drilled following σ_h and σ_H (Seyedi et al 2017). However, those models are limited in 2D modeling, which cannot show some 3D effect on the claystone response, for instance: the delay of convergence at different sections, the pore pressure distribution at the drift front, etc.

This study focuses on developing a nonlinear model including both the elastic anisotropy and the induced anisotropic plasticity. The basic assumption is that the failure of an anisotropic material is due to either fracturing of weakness planes (ubiquitous joints) and the failure of the rock matrix. The ubiquitous joints are introduced based on the orientation of the induced fractures to reproduce the induced anisotropy. Thus, the rock is composed of a matrix and of potential weakness planes as observed from the biaxial tests under plane strain conditions. The proposed model is implemented in *FLAC3D* (Itasca 2017). Comparisons with in-situ observations on two drifts within the URL, namely GCS and GED drilled following two directions of σ_H and σ_h, were made. Analysis is focused on the excavation induced the fractured zones and the gallery convergence.

2 CONSTITUITIVE MODEL AND IMPLEMENTATION

The rock matrix is described as an elastoplastic model in which the elasticity is linear and transversely isotropic, and the plasticity is formulated from a generalization Hoek-Brown yield criterion and a non-associated flow rule. The constitutive equations describing the rheological model for COx claystone consists of the plastic yield functions for shear and tensile regimes F_s^m, F_t^m and a non-associated plastic potential for shear plasticity G_s^m and an associated rule flow for tensile plasticity G_t^m.

$$F_s^{\,m} = \frac{4}{3}\frac{\cos^2\theta}{A}q^2 + \left(\frac{\cos\theta}{\sqrt{3}} - \frac{\sin\theta}{3}\right)q + p - \frac{B}{A} \tag{1}$$

$$F_t^{\,m} = p - \sigma_t \tag{2}$$

$$G_s^{\,m} = q + \beta(\gamma)p \tag{3}$$

in which

$$\beta(\gamma) = \begin{cases} \beta_m - (\beta_m - \beta_0)e^{-b_\beta \gamma} & \text{si } \gamma \le \gamma^{ult} \\ \beta_{ult} e^{\left(1 - \gamma/\gamma^{ult}\right)} & \gamma > \gamma^{ult} \end{cases} \tag{4}$$

$$\beta_{ult} = \beta_m - \beta_m(\beta_m - \beta_0)e^{-b_\beta \gamma^{ult}} \tag{5}$$

where θ is the Lode's angle; p the mean stress; q the deviatoric stress; $A = m\sigma_c$; $B = s\sigma_c^2$; m and s Hoek and Brown criterion parameters; σ_c the uniaxial compressive strength; σ_t the tensile strength; $\beta(\gamma)$ the rate of dilatancy; γ the plastic distortion (internal flow variable) varying from a minimum value β_0 and a maximum value β_{ult} according to Equation 5; b_β the plastic flow velocity; γ^{ult} the ultimate deformation from which the dilatancy begins to decrease, to completely disappear with the increase of plastic strain.

The strain hardening in pre-peak and the strain softening in post-peak are modelled as monotonic parabolic evolutions (without introducing new parameters) of A and B versus γ is considered from the initiation of plasticity to peak (hardening stage) and from the peak to the residual strength (softening stage). For residual strength, the yield function (1) is suitable if the confining pressure does not exceed the transition stress between the brittle and ductile behavior σ_3^{bd}. Beyond this confining stress, residual strength has the same form of the yield function at the peak. The relation between the parameters at the peak and at the beginning of residual stage is

$$m_r = m_p + \left(s_p - s_r\right)\frac{\sigma_c}{\sigma_3^{\,bd}} \tag{6}$$

Details of the proposed model and its calibration/validation against laboratory tests for the COx claystone can be referred by Souley et al 2017.

Induced fracture is modelled as the ubiquitous joint assumed to be elastic perfectly plastic with the Mohr-Coulomb criterion. The orientation of the weakness plane is determined based on the fundamental linear fracture mechanic. Failure experiments on the brittle material exhibit two fracture modes I and II. The mode I is the case of tensile/extension facture occurring when the minimum principal stress σ_3 reaches the tensile stress or close to zero as in uniaxial compression (longitudinal splitting). The fracture is perpendicular to the minimal principal stress direction. The mode II consists in the shear facture under triaxial compression condition, for which two conjugate fractures, with angle $\Theta = \pm(\pi/4 - \phi_{wp}/2)$ (ϕ_{wp} the friction angle along the weakness plane) with respect to the maximum compressive stress, initiate and grow. It is worth noting that the fundamental difference with the implementation of ubiquitous joints in the Itasca codes is the fact that the orientation of the weakness plane is not imposed, even if we have left (in optional) the possibility of predefined directions of ubiquitous joints.

The constitutive equations for the weakness plane are established in the local system ($\underline{s},\underline{t},\underline{n}$) where ($\underline{s},\underline{t}$) is the weakness plane and $\underline{n}$ its unit normal. The yield and potential functions read

$$\begin{cases} F_s^{\,wp} = \tau + \sigma_{nn}\tan\phi_{wp} - C_{wp} \\ F_t^{\,wp} = \sigma_{nn} - \sigma_t^{wp} \end{cases} \tag{7}$$

$$\begin{cases} G_s^{\,wp} = \tau + \sigma_{nn}\tan\psi \\ G_t^{\,wp} = \sigma_{nn} \end{cases} \tag{8}$$

where ϕ_{wp}, C_{wp}, ψ_{wp}, σ_{wp}^{t} are the friction angle, cohesion, mobilized dilation angle and tensile strength of the weakness plane; τ and γ_{wp} are defined by

$$\tau = \sqrt{{\sigma_{sn}}^2 + {\sigma_{tn}}^2} \quad \text{and} \quad \gamma^{wp} = \sqrt{{\varepsilon_{sn}}^2 + {\varepsilon_{tn}}^2} \tag{10}$$

The angle of dilatancy ψ remains constant and equal to ψ_{wp} up to a shear plastic strain along weakness plane of γ^{ult}. Beyond γ^{ult}, it decreases exponentially to reach 0 (Eq. 5).

The previous constitutive equations have been implemented in *FLAC3D* under the option UDM (C++ User Defined Model) available in Itasca codes. The main flowchart of the implementation is summarized below.

- The first approximation of stress tensor $\underline{\sigma}^{i}$, is evaluated by adding to the previous stress tensor the stress increment computed from the total strain increments and the Hooke's law.
- Computation of the yield function for rock matrix, $F^m(p^i, q^i, \theta^i)$ according to Equations 1 & 2. If the stress state, $\underline{\sigma}^{i}$, satisfies the yield criterion: $F^m(p^i, q^i, \theta^i) > 0$, the new increment of stresses is computed as well as the new stress tensor, $\underline{\sigma}^{o}$. If $F^m(p^i, q^i, \theta^i) \leq 0$, the current stress components are: $\underline{\sigma}^{o} = \underline{\sigma}^{i}$.

The resulting stress tensor, $\underline{\sigma}^{o}$, is then examined for failure on the weak plane.

- The corresponding stress components in the local axes, $\underline{\sigma}'^{o}$, are computed using the transformation from global system (x,y,z) to the local one ($\underline{s}$,$\underline{t}$,$\underline{n}$).
- Computation of the yield function for weak plane, $F^{wp}(\sigma_{nn}'^{o}, \tau'^{o})$ according to Equation 6. If the stress state $\underline{\sigma}'^{o}$ verifies the yield criterion $F^{wp}(\sigma_{nn}'^{o}, \tau'^{o}) > 0$, the new increment of stresses is computed as well as the new stress tensor, $\underline{\sigma}^{n}$. If $F^{wp}(\sigma_{nn}'^{o}, \tau'^{o}) \leq 0$, the current new stresses are: $\underline{\sigma}^{n} = \underline{\sigma}'^{o}$.
- Back to global system (x,y,z), $\underline{\sigma}^{n}$.
- Parameters depending on the internal plastic variable are updated.

3 RESULTS AND DISCUSSION

The present model has been first calibrated/validated against the laboratory test, secondly used to reproduce the in-situ mechanical observation during the drilling phase of different galleries within the URL. This section is devoted to describing the claystone response due to the excavation for two drifts GCS and GED. The gallery GCS was drilled following the direction of major horizontal stress (σ_H), thus, the initial total stress is quasi-isotropic in the gallery section ($\sigma_v \approx \sigma_h$). Measurement exhibits an anisotropic form of the fractured zone with e_h/e_v~2.4-3.0 (e_h, e_v are the horizontal and vertical extents of the fractured zone from the gallery center) and an anisotropic convergence with the ratio c_h/c_v~1.5-2.0 (c_h, c_v are the horizontal and vertical convergences). The gallery GED is oriented following σ_h and hence the initial total stress is anisotropic in its section ($\sigma_H > \sigma_v \approx \sigma_h$). The excavation of GED gallery induced a fractured zone with e_v/e_h~2.0-3.2 and the convergence ratio c_v/c_h~3-4. The conceptual model of the fractured zones around these two galleries is shown in Figure 1 (Armand et al. 2014).

3D modeling of two galleries GCS and GED using the proposed model is performed respecting the real geometries and the real excavation stages. Figure 2 displays the plastic zones around these two galleries due to the drilling. The results show a horizontal extension of softening and residual behavior zone around the gallery GCS and a vertical extension for the gallery GED, which are in accordance with the conceptual model built from in-situ data. The convergence obtained by the present model shows an anisotropy with c_h/c_v~1.6-2 for different sections of GCS and c_v/c_h~3-4 for different sections of GED (see Fig. 3). Moreover, the absolute value of convergence and its delay due to the excavation step are in a good agreement with the in-situ observation reported by Armand et al. 2013.

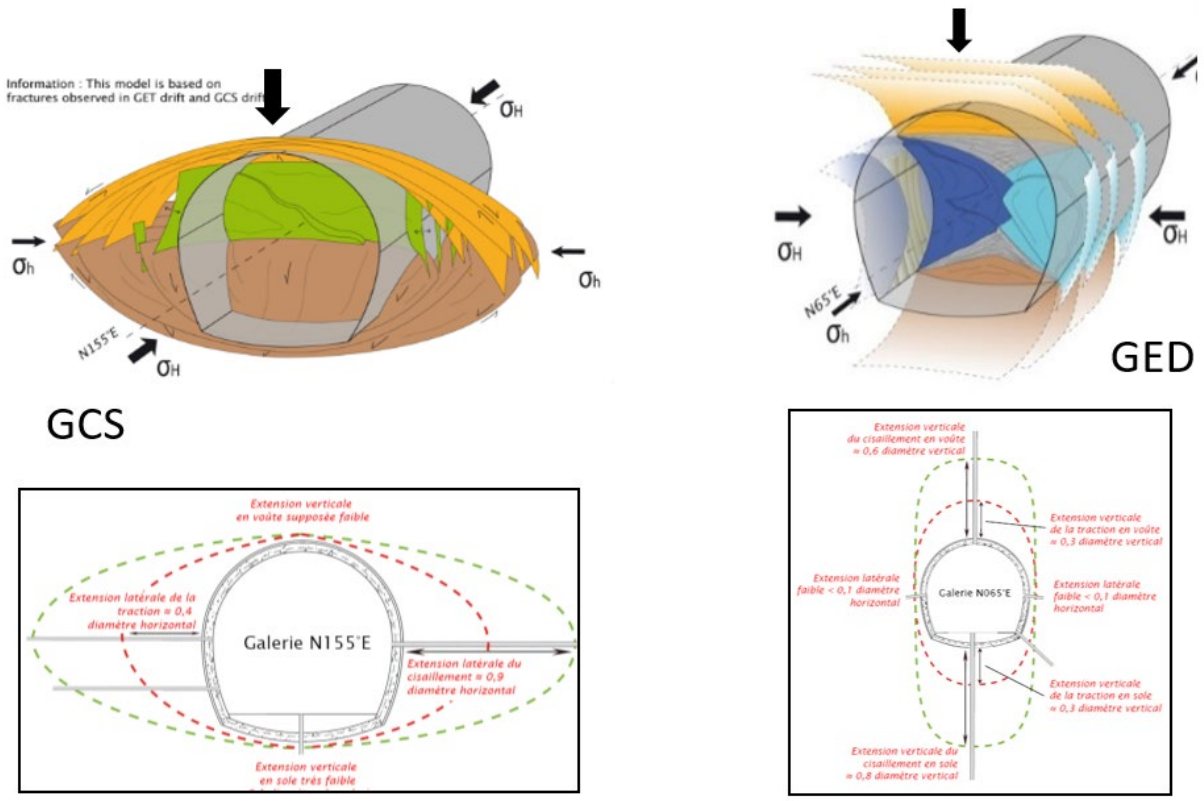

Figure 1. Conceptual model of fractured zones around two galleries GCS and GED.

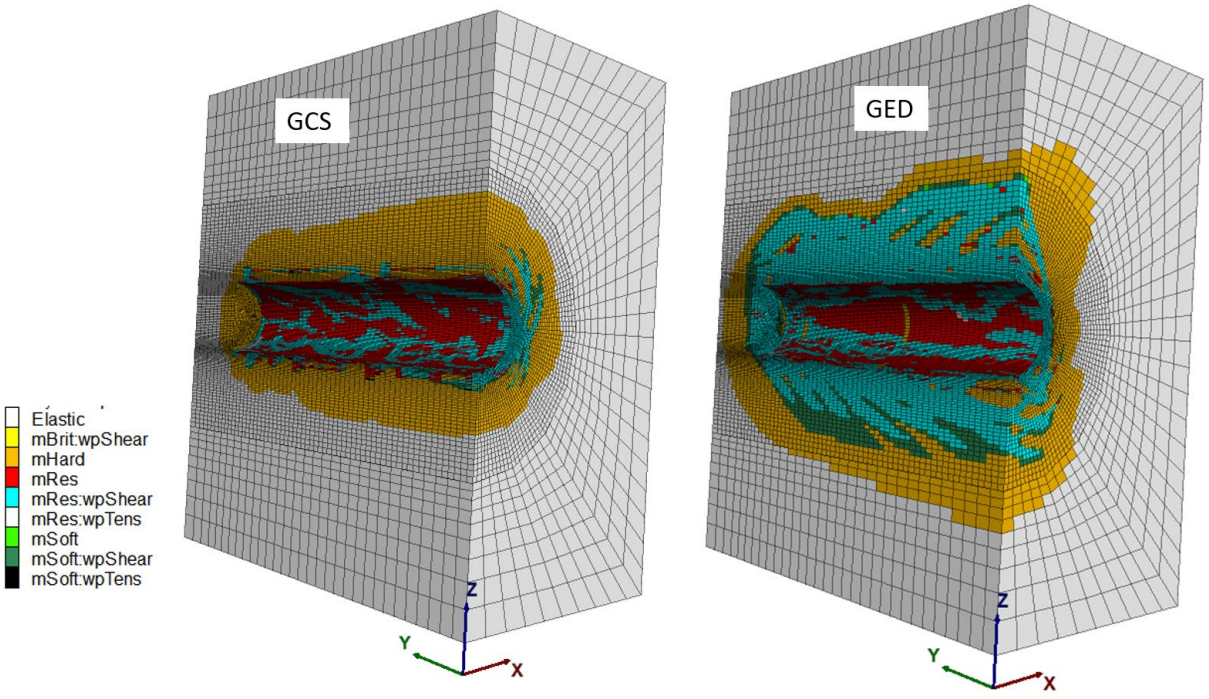

Figure 2. Modeling of plastic zones of two galleries GCS and GED.

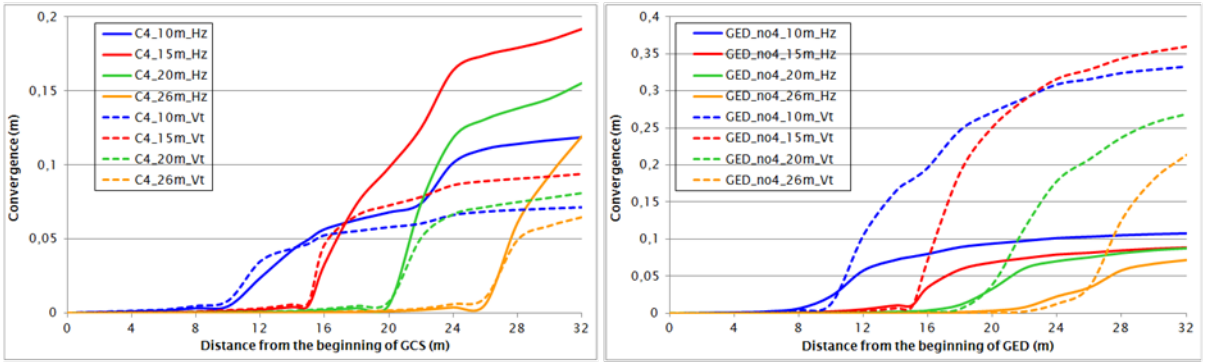

Figure 3. Convergences of two galleries GCS and GED during excavation.

4 CONCLUSIONS

An elastoplastic model is proposed in this paper to model the induced anisotropy observed when excavating different drifts in the URL at Meuse/Haute-Marne, based on the ubiquitous joints. The failure of the claystone is due to the failure of the rock matrix and/or the failure along the weakness plan. The weakness plane direction is introduced with respect to the fundamental linear fracture mechanic, which can be tensile/extension or shear fractures. The proposed model shows a good agreement with experimental data tests on the sample and from the URL. The introduction of long-term behavior of both the intact rock and the weakness plane is an ongoing work.

REFERENCES

Armand, G., Leveau. F., Nussbaum, C., de La Vaissiere, R., Noiret, A., Jaeggi, D., Landrein, P. & Righini, C. 2014. Geometry and properties of the excavation induced fractures at the Meuse/Haute-Marne URL drifts. *Rock Mechanics and Rock Engineering* 47: 21-41.

Armand, G., Noiret, A., Zghondi, J. & Seyedi, D. 2013. Short-and long-term behaviors of drifts in the Callovo-Oxfordian claystone at the Meuse/Haute-Marne Underground Research Laboratory. *Journal of Rock Mechanics and Geotechnical Engineering* 5(3): 221-230.

Itasca Consulting Group, Inc. 2017. *FLAC3D – Fast Lagrangian Analysis of Continua in Three-Dimensions, Ver. 6.0*. Minneapolis: Itasca.

Seyedi, D., Armand, G. & Noiret, A. 2017. "Transverse Action"–A model benchmark exercise for numerical analysis of the Callovo-Oxfordian claystone hydromechanical response to excavation operations. *Computers and Geotechnics* 85: 287-305.

Souley, M., Armand, G. & Kazmierczak, J.B. 2017. Hydro-elasto-viscoplastic modeling of a drift at the Meuse/Haute-Marne Underground Research Laboratory (URL). *Computers and Geotechnics* 85: 306-320.